



**UNIVERSITI PUTRA MALAYSIA**

**PHYSICAL AND ELECTRICAL PROPERTIES OF BISMUTH STRONTIUM  
OXIDE - BASED SOLID SOLUTIONS**

**ROHAYU BT MOHD NOOR**

**FS 2019 7**



**PHYSICAL AND ELECTRICAL PROPERTIES OF BISMUTH STRONTIUM  
OXIDE - BASED SOLID SOLUTIONS**

By

**ROHAYU BINTI MOHD NOOR**

**Thesis submitted to the School of Graduate Studies, Universiti Putra Malaysia, in  
Fullfilment of the Requirements for the Degree of Master of Science**

**April 2019**

All material contained within the thesis, including without limitation text, logos, icons, photographs and all other artwork, is copyright material of Universiti Putra Malaysia unless otherwise stated. Use may be made of any material contained within the thesis for non-commercial purposes from the copyright holder. Commercial use of material may only be made with the express, prior, written permission of Universiti Putra Malaysia.

Copyright © Universiti Putra Malaysia



Abstract of thesis presented to the Senate of Universiti Putra Malaysia in fulfillment of the requirement for the degree of Master of Science

## PHYSICAL AND ELECTRICAL PROPERTIES OF BISMUTH STRONTIUM OXIDE - BASED SOLID SOLUTIONS

By

ROHAYU BINTI MOHD NOOR

April, 2019

Chair: Tan Yen Ping, PhD  
Faculty: Science

Bismuth oxide systems exhibit high oxide ion conductivity and have been proposed as good electrolyte materials. However, due to their instability under conditions of low oxygen partial pressures there has been difficulty in developing these materials and thus, strontium is introduced in order to overcome this problem. The bismuth strontium oxide ( $\text{Bi}_{2-2x}\text{Sr}_x\text{O}_{3-2x}$ ) where  $0.1 \leq x \leq 0.8$  is synthesized via conventional solid state method at  $800^\circ\text{C}$  for 24-48 hours. X-ray diffraction studies revealed that the single phase hexagonal structure with space group of R-3m and lattice parameter of  $a=b \neq c$  is attained in composition of  $0.1 \leq x \leq 0.4$ . Mixed phases were obtained for the composition of  $0.5 \leq x \leq 0.8$  and therefore, it can be concluded that the solid solution limit for this material is in the composition of  $0.1 \leq x \leq 0.4$ . The electrical properties were studied using AC impedance in the frequency range of 0.1 Hz – 1 MHz at temperature of  $25-800^\circ\text{C}$ . At temperature  $200-400^\circ\text{C}$ ,  $\text{Bi}_{2-2x}\text{Sr}_x\text{O}_{3-2x}$  solid solutions were having an oxide ionic conduction with conductivity  $\sim 10^{-6} - 10^{-1} \text{ Scm}^{-1}$  while the activation energies,  $E_a$  were in the range of 0.76-1.12 eV.

Chemical doping using divalent cations were carried out on the  $\text{Sr}^{2+}$  site with selected dopants i.e. manesium oxide (MgO), calcium oxide (CaO), barium oxide (BaO) and nickel oxide (NiO) in order to modify and enhance the electrical properties of the material and all dopants were introduced into  $\text{Bi}_{1.2}\text{Sr}_{0.4}\text{O}_{2.2}$ . The divalent dopants are introduced at  $\text{Sr}^{2+}$  site because of its comparable ionic radius to  $\text{Sr}^{2+}$ . The single phase pure of these samples were determine by using the X-ray diffraction method (XRD). The solid solution limit for Mg-doped ( $\text{Bi}_{1.2}\text{Sr}_{0.4-x}\text{Mg}_x\text{O}_{2.2}$ ) is  $0.00 \leq x \leq 0.10$  meanwhile, solid solution limit for Ca-doped ( $\text{Bi}_{1.2}\text{Sr}_{0.4-x}\text{Ca}_x\text{O}_{2.2}$ ) is  $0.00 \leq x \leq 0.08$ . The solid solution limit for Ba-doped ( $\text{Bi}_{1.2}\text{Sr}_{0.4-x}\text{Ba}_x\text{O}_{2.2}$ ) is in the range of  $0.00 \leq x \leq 0.06$  and as for the Ni-doped ( $\text{Bi}_{1.2}\text{Sr}_{0.4-x}\text{Ni}_x\text{O}_{2.2}$ ) the solid solution limit is  $0.00 \leq x \leq 0.10$ . All of these doped materials are in hexagonal structure with space group of R-3m.

At temperature of 200-400°C the ionic conductivity for  $\text{Bi}_{1.2}\text{Sr}_{0.4-x}\text{Mg}_x\text{O}_{2.2}$  solid solutions are  $10^{-6}$ - $10^{-1} \text{ Scm}^{-1}$  with activation energy in the range of 0.93-0.97 eV. The  $\text{Bi}_{1.2}\text{Sr}_{0.3}\text{Mg}_{0.1}\text{O}_{2.2}$  has the highest conductivity of  $1.23 \times 10^{-1} \text{ Scm}^{-1}$  at 400°C. An increase in conductivity was observed as the composition of Ca-doped increased; at temperature of 200-400°C is in the range of  $10^{-6}$ - $10^{-2} \text{ Scm}^{-1}$  with activation energy in the range of 0.96-1.14 eV. The  $\text{Bi}_{1.2}\text{Sr}_{0.32}\text{Ca}_{0.08}\text{O}_{2.2}$  has the highest conductivity at 400°C which is  $5.62 \times 10^{-2} \text{ Scm}^{-1}$  and  $E_a$  is 1.14 eV. The conductivity decreased as the amount of  $\text{Ba}^{2+}$  increases. The ionic conductivity at temperature of 200-400°C is  $10^{-6}$ - $10^{-2} \text{ Scm}^{-1}$  and  $E_a$  is 0.89-1.10 eV. The  $\text{Bi}_{1.2}\text{Sr}_{0.36}\text{Ba}_{0.04}\text{O}_{2.2}$  is having high conductivity of  $5.33 \times 10^{-2} \text{ Scm}^{-1}$  at 400°C as compared to the  $\text{Bi}_{1.2}\text{Sr}_{0.4}\text{O}_{2.2}$ . The ionic conductivity of Ni-doped at temperature of 200-400°C is  $10^{-6}$ - $10^{-2} \text{ Scm}^{-1}$  with the activation energy of 0.69-1.07 eV. The  $\text{Bi}_{1.2}\text{Sr}_{0.38}\text{Ni}_{0.02}\text{O}_{2.2}$  has the highest conductivity of  $2.88 \times 10^{-2} \text{ Scm}^{-1}$  at 400°C.

The atomic percent of elements present in all samples were confirmed by using the energy dispersive X-ray spectroscopy (EDX). Surface morphology of these samples was viewed using the scanning electron microscopy (SEM).

Abstrak tesis yang dikemukakan kepada Senat Universiti Putra Malaysia sebagai memenuhi keperluan untuk Ijazah Sarjana Sains

## SIFAT FIZIKAL DAN ELEKTRIK BAGI BISMUTH STRONTIUM OKSIDA - BERASASKAN LARUTAN PEPEJAL

Oleh

ROHAYU BINTI MOHD NOOR

April 2019

**Pengerusi: Tan Yen Ping, PhD**  
**Fakulti: Sains**

Sistem oksida Bismuth menunjukkan kekonduksian ion oksida yang tinggi dan telah dicadangkan sebagai bahan elektrolit yang baik. Walau bagaimanapun, disebabkan oleh ketidakstabilan mereka dalam keadaan tekanan separa oksigen yang rendah, terdapat kesukaran untuk membangunkan bahan-bahan ini dan dengan demikian, strontium diperkenalkan untuk mengatasi masalah ini. Strontium oksida bismut ( $\text{Bi}_{2-2x}\text{Sr}_x\text{O}_{3-2x}$ ) di mana  $0.1 \leq x \leq 0.8$  disintesis melalui kaedah keadaan pepejal konvensional pada  $800^\circ\text{C}$  selama 24-48 jam. Kajian difraksi sinar-X mendedahkan bahawa fasa tunggal struktur heksagon dengan kumpulan ruang R-3m dan parameter kekisi  $a = b \neq c$  dicapai dalam komposisi  $0.1 \leq x \leq 0.4$ . Fasa campuran diperolehi untuk komposisi  $0.5 \leq x \leq 0.8$  dan oleh itu, dapat disimpulkan bahawa had larutan pepejal untuk bahan ini adalah dalam komposisi  $0.1 \leq x \leq 0.4$ . Ciri-ciri elektrik telah dikaji menggunakan impedans AC dalam julat kekerapan 0.1 Hz - 1 MHz pada suhu  $25-800^\circ\text{C}$ . Pada suhu  $200-400^\circ\text{C}$ , penyelesaian pepejal  $\text{Bi}_{2-2x}\text{Sr}_x\text{O}_{3-2x}$  mempunyai pengaliran ionik oksida dengan kekonduksian  $\sim 10^{-6}-10^{-1} \text{ Scm}^{-1}$  manakala tenaga pengaktifan,  $E_a$  berada dalam lingkungan 0.76-1.12 eV.

Doping kimia menggunakan kation divalen dilakukan di tapak  $\text{Sr}^{2+}$  dengan dopan terpilih iaitu magnesium oksida ( $\text{MgO}$ ), kalsium oksida ( $\text{CaO}$ ), barium oksida ( $\text{BaO}$ ) dan nikel oksida ( $\text{NiO}$ ) untuk mengubahsuaikan dan meningkatkan sifat-sifat elektrik bahan dan semua dopan diperkenalkan ke dalam  $\text{Bi}_{1.2}\text{Sr}_{0.4}\text{O}_{2.2}$ . Dopan divalen diperkenalkan di tapak  $\text{Sr}^{2+}$  kerana radius ionik setanding kepada  $\text{Sr}^{2+}$ . Fasa tunggal murni sampel ini ditentukan dengan menggunakan kaedah difraksi sinar-X (XRD). Had larutan pepejal untuk Mg-doped ( $\text{Bi}_{1.2}\text{Sr}_{0.4-x}\text{Mg}_x\text{O}_{2.2}$ ) ialah  $0.00 \leq x \leq 0.10$  sementara itu, had larutan pepejal untuk Ca-doped ( $\text{Bi}_{1.2}\text{Sr}_{0.4-x}\text{Ca}_x\text{O}_{2.2}$ ) ialah  $0.00 \leq x \leq 0.08$ . Had larutan pepejal untuk Ba-doped ( $\text{Bi}_{1.2}\text{Sr}_{0.4-x}\text{Ba}_x\text{O}_{2.2}$ ) berada dalam lingkungan  $0.00 \leq x \leq 0.06$  dan bagi Ni-doped ( $\text{Bi}_{1.2}\text{Sr}_{0.4-x}\text{Ni}_x\text{O}_{2.2}$ ) penyelesaian pepejal had ialah  $0.00 \leq x \leq 0.10$ . Semua bahan doped ini berada dalam struktur heksagon dengan kumpulan ruang R-3m.

Pada suhu 200-400°C, kekonduksian ionik untuk penyelesaian pepejal  $\text{Bi}_{1.2}\text{Sr}_{0.4-x}\text{Mg}_x\text{O}_{2.2}$  adalah  $10^{-6}$ - $10^{-1} \text{ Scm}^{-1}$  dengan tenaga pengaktifan dalam julat 0.93-0.97 eV.  $\text{Bi}_{1.2}\text{Sr}_{0.3}\text{Mg}_{0.1}\text{O}_{2.2}$  mempunyai kekonduksian tertinggi  $1.23 \times 10^{-1} \text{ Scm}^{-1}$  pada 400°C. Peningkatan kekonduksian diperhatikan kerana komposisi Ca-doped meningkat; pada suhu 200-400°C adalah dalam lingkungan  $10^{-6}$ - $10^{-2} \text{ Scm}^{-1}$  dengan tenaga pengaktifan dalam julat 0.96-1.14 eV.  $\text{Bi}_{1.2}\text{Sr}_{0.32}\text{Ca}_{0.08}\text{O}_{2.2}$  mempunyai kekonduksian tertinggi pada 400°C iaitu  $5.62 \times 10^{-2} \text{ Scm}^{-1}$  dan  $E_a$  adalah 1.14 eV. Konduktiviti menurun apabila jumlah peningkatan  $\text{Ba}^{2+}$  meningkat. Kekonduksian ionik pada suhu 200-400 °C ialah  $10^{-6}$ - $10^{-2} \text{ Scm}^{-1}$  dan  $E_a$  adalah 0.89-1.10 eV.  $\text{Bi}_{1.2}\text{Sr}_{0.36}\text{Ba}_{0.04}\text{O}_{2.2}$  mempunyai kekonduksian tinggi  $5.33 \times 10^{-2} \text{ Scm}^{-1}$  pada 400°C berbanding dengan  $\text{Bi}_{1.2}\text{Sr}_{0.4}\text{O}_{2.2}$ . Kekonduksian ionik Ni-doped pada suhu 200-400°C adalah  $10^{-6}$ - $10^{-2} \text{ Scm}^{-1}$  dengan tenaga pengaktifan 0.69-1.07 eV.  $\text{Bi}_{1.2}\text{Sr}_{0.38}\text{Ni}_{0.02}\text{O}_{2.2}$  mempunyai kekonduksian tertinggi pada  $2.88 \times 10^{-2} \text{ Scm}^{-1}$  pada 400°C.

Persentase atom unsur dalam semua sampel telah disahkan menggunakan spektroskopi X-ray dispersif tenaga (EDX). Morfologi permukaan sampel ini dilihat menggunakan mikroskop elektron imbasan (SEM).

## ACKNOWLEDGEMENTS

First of all I would like to express my truly appreciation and deep gratitude to my supervisor, Dr. Tan Yen Ping for her guidance, constructive comments, patience, continuous support, kindness and invaluable advice and suggestions throughout the duration of this study. I extend my sincere appreciation to my co-supervisor Assoc. Prof. dr. Tan Kar Ban for his guidance, suggestion and comments throughout the research work. Their credits are always appreciated and never forgotten.

I would like to thank the UPM Chemistry Department staff especially Puan Zaidina (XRD), and Puan Farah (SEM and EDX) for their technical assistance and guidance in operating the instruments. I would like to express my gratitude to my lab senior Miss Kartika Firman for her patience and guidance for my research study and I also like to thank all my lab mates and friends, Syafiqah, Krishana, Farah and Vivian for their endless support and providing me with laughter and joy all the way through.

The financial support from the Ministry of Science and Technology and University Putra Malaysia is gratefully acknowledged. Without this support, it is impossible for me to pursue this project with success. Last but not least, my deepest affection and gratitude to my beloved family members for their love, continuous support, encouragement and understanding throughout the period of my study.



I certify that a Thesis Examination Committee has met on 22 April 2019 to conduct the final examination of Rohayu Binti Mohd Noor on her thesis entitled “Physical and Electrical Properties of Bismuth Strontium Oxide - Based Solid Electrolytes” in accordance with the Universities and University Colleges Act 1971 and the Constitution of the University Putra Malaysia [P.U. (A) 106] 15 March 1998. The committee recommends that the student be awarded the degree of Master of Science.

Members of the Thesis Examination Committee were as follows:

**Norhazlin binti Zainuddin, PhD**

Senior Lecturer  
Faculty of Science  
University Putra Malaysia  
(Chairman)

**Rusniza Binti Mohd Zawawi, PhD**

Senior Lecturer  
Faculty of Science  
University Putra Malaysia  
(Internal Examiner)

**Noor Haida Bin Mohd Kaus, PhD**

Senior Lecturer  
School of Chemical Sciences  
Universiti Sains Malaysia  
(External Examiner)

---

**RUSLI HAJI ABDULLAH, PhD**

Professor/Dean  
School of Graduate Studies  
Universiti Putra Malaysia

Date:

This thesis was submitted to the Senate of Universiti Putra Malaysia and has been accepted as fulfillment of the requirement for the degree of Master of Science. The members of the Supervisory Committee were as follows:

**Tan Yen Ping, PhD**

Senior Lecturer  
Faculty of Science  
Universiti Putra Malaysia  
(Chairman)

**Tan Kar Ban, PhD**

Associate Professor  
Faculty of Science  
Universiti Putra Malaysia  
(Member)

---

**ROBIAH BINTI YUNUS, PhD**

Professor and Dean  
School of Graduate Studies  
Universiti Putra Malaysia

Date:

## Declaration by graduate students

I hereby declare that:

- this thesis is my original work;
- quotations, illustrations and citations have been duly referenced;  
this thesis has not been submitted previously or currently for any other degree at any other institutions;
- intellectual property from the thesis and copyright of thesis are fully-owned by Universiti Putra Malaysia, as according to the Universiti Putra Malaysia (Research) Rules 2012;
- written permission must be obtained from supervisor and the office of Deputy Vice-Chancellor (Research and Innovation) before thesis is published (in the form of written, printed, or in electronic form) including books, journals, modules, proceedings, popular writings, seminar papers, manuscripts, posters, reports, lecture notes, learning modules, or any other materials as stated in the Universiti Putra Malaysia (Research) Rules 2012;
- there is no plagiarism or data falsification/ fabrication in the thesis, and scholarly integrity is upheld as according to the Universiti Putra Malaysia (Graduate Studies) Rules 2003 (Revision 2012-2013) and the Universiti Putra Malaysia (Research) Rules 2012. The thesis has undergone plagiarism detection software.

Signature: \_\_\_\_\_

Date: \_\_\_\_\_

Name and Matric No: Rohayu binti Mohd Noor, GS44702

## Declaration by Members of Supervisory Committee

This is to confirm that:

- the research conducted and the writing of this thesis was under our supervision;
- supervision responsibilities as stated in the Universiti Putra Malaysia (Graduate Studies) Rules 2003 (Revision 2012-2013) are adhered to:

Signature: \_\_\_\_\_

Name of Chairman of Supervisory Committee: Tan Yen Ping

Signature: \_\_\_\_\_

Name of Member of Supervisory Committee: Tan Kar Ban

## TABLE OF CONTENTS

	<b>Page</b>
<b>ABSTRACT</b>	i
<b>ABSTRAK</b>	iii
<b>ACKNOWLEDGEMENTS</b>	vi
<b>APPROVAL</b>	vii
<b>DECLARATION</b>	viii
<b>LIST OF TABLES</b>	xii
<b>LIST OF FIGURES</b>	xiv
<b>LIST OF ABBREVIATIONS</b>	xviii
<b>CHAPTER</b>	
<b>1. INTRODUCTION</b>	
1.1 Overview	1
1.2 Solid Electrolytes	2
1.3 Oxide Ion Conductors	3
1.4 Ionic Conductivity	3
1.5 Application of Ionic Conduction	5
1.5.1 Solid Oxide Fuel Cells (SOFC's)	5
1.6 Problem Statements	7
1.7 Objectives	8
<b>2. LITERATURE REVIEW</b>	
2.1 Bismuth Oxide ( $\text{Bi}_2\text{O}_3$ )	9
2.1.1 The structure of $\alpha$ - $\text{Bi}_2\text{O}_3$	10
2.1.2 The structure of $\delta$ - $\text{Bi}_2\text{O}_3$	10
2.1.3 The structure of $\beta$ and $\gamma$ - $\text{Bi}_2\text{O}_3$	11
2.2 Electrical Properties of $\text{Bi}_2\text{O}_3$	12
2.3 Doped Bismuth Oxide, $\text{Bi}_2\text{O}_3$	14
2.3.1 Bismuth Strontium Oxide ( $\text{Bi}_2\text{O}_3$ -SrO)	14
2.3.1.1 Structure of $\text{Bi}_2\text{O}_3$ - SrO	15
2.3.1.2 Conductivity of $\text{Bi}_2\text{O}_3$ - SrO	16
2.3.2 Introduction of Dopants $\text{Bi}_2\text{O}_3$ - SrO	17
<b>3. MATERIALS AND METHOD</b>	
3.1 Bismuth Strontium Oxide Preparation	22
3.2 Preparation of Doped Bismuth Strontium Oxide	24
3.3 Pellet Preparation	24
3.4 Characterization of Samples	24
3.4.1 X-ray Diffraction (XRD)	25
3.4.2 Energy-dispersive X-ray Spectroscopy (EDX)	26
3.4.3 Scanning Electron Microscopy (SEM)	26
3.5 Electrical Properties	27

3.5.1 AC Impedance Spectroscopy	27
3.5.2 Cole-cole Plot	27
3.5.3 Modulus Spectroscopy	29
<b>4. RESULTS AND DISCUSSION</b>	
4.1 The bismuth strontium oxide solid solutions	32
4.1.1 Phase Formation	33
4.1.2 Crystallite Size Studies	36
4.1.3 Elemental Analysis and Surface Morphology	39
4.1.4 AC Impedance Analysis	41
4.2 Doped Bismuth Strontium solid solutions	48
4.2.1 Phase Formation	49
4.2.2 Crystallite Size Studies	58
4.2.3 Elemental Analysis and Surface Morphology	64
4.2.4 AC Impedance Analysis	72
<b>5. CONCLUSION</b>	93
<b>FURTHER WORK</b>	94
<b>REFERENCES</b>	95
<b>APPENDICES</b>	99
<b>BIODATA OF STUDENT</b>	104

## LIST OF TABLES

Table	Page	
2.1	Bi <sub>2</sub> O <sub>3</sub> phase transition temperature, °C (Sammes <i>et.al.</i> , 1999)	10
2.2	Structural data of the Bi <sub>2</sub> O <sub>3</sub> phases (Harwig, 1978)	12
2.3	Conductivity parameters observed for Bi <sub>2</sub> O <sub>3</sub> phases.	14
2.4	Summarize of the lattice parameter and structure for the different composition of bismuth strontium oxide (Bi <sub>2</sub> O <sub>3</sub> -SrO)	15
2.5	The summary of the crystal structure and space group for the doped Fe	18
2.6	Bi <sub>1-x</sub> Sr <sub>x</sub> FeO <sub>3</sub> (x=0.00, 0.02, 0.10, 0.20 and 0.30), Bi <sub>1-x</sub> Sr <sub>x</sub> FeO (x=0.40, 0.45, and 0.50) and SrBi <sub>x</sub> Fe <sub>12-x</sub> O <sub>19</sub> (0.00 ≤ x ≤ 1.0)	18
2.7	Activation energy of Bi <sub>1-x</sub> Sr <sub>x</sub> FeO <sub>3</sub> (0.40 ≤ x ≤ 0.55) (Thakur <i>et.al.</i> , 2014)	19
2.8	The summary of the dopants used in the bismuth strontium oxide with the X-ray diffraction data (XRD)	21
3.1	Capacitance values and their possible interpretation	29
4.1	The summary of compositions, phases and sintering conditions for Bi <sub>2-2x</sub> Sr <sub>x</sub> O <sub>3-2x</sub> (0.1 ≤ x ≤ 0.6)	35
4.2	Calculated grain sizes, crystallite sizes and internal strains	38
4.3	The atomic percentage by EDX analysis for Bi <sub>2-2x</sub> Sr <sub>x</sub> O <sub>3-2x</sub> (0.1 ≤ x ≤ 0.4) solid solutions	40
4.4	Ionic conductivity for Bi <sub>2-2x</sub> Sr <sub>x</sub> O <sub>3-2x</sub> where (0.1 ≤ x ≤ 0.4) at different temperature	48
4.5	Summary of compositions, treatment conditions and phases for the doped materials	55
4.6	The atomic percentage by EDX analysis for Bi <sub>1.2</sub> Sr <sub>0.4-x</sub> Mg <sub>x</sub> O <sub>2.2</sub> (0.00 ≤ x ≤ 0.10) solid solutions	59
4.7	The atomic percentage by EDX analysis for Bi <sub>1.2</sub> Sr <sub>0.4-x</sub> Ca <sub>x</sub> O <sub>2.2</sub> (0.00 ≤ x ≤ 0.08) solid solutions	61
4.8	The atomic percentage by EDX analysis for Bi <sub>1.2</sub> Sr <sub>0.4-x</sub> Ba <sub>x</sub> O <sub>2.2</sub> (0.00 ≤ x ≤ 0.06) solid solutions	62

4.9	The atomic percentage by EDX analysis for $\text{Bi}_{1.2}\text{Sr}_{0.4-x}\text{Ba}_x\text{O}_{2.2}$ ( $0.00 \leq x \leq 0.06$ ) solid solutions	64
4.10	The summary for the crystallite sizes and internal strain for $\text{Bi}_{1.2}\text{Sr}_{0.4-x}\text{Mg}_x\text{O}_{2.2}$ ( $0.00 \leq x \leq 0.10$ ) solid solutions	65
4.11	The summary for the crystallite sizes and internal strain for $\text{Bi}_{1.2}\text{Sr}_{0.4-x}\text{Ca}_x\text{O}_{2.2}$ ( $0.00 \leq x \leq 0.08$ ) solid solutions	66
4.12	The summary for the crystallite sizes and internal strain for $\text{Bi}_{1.2}\text{Sr}_{0.4-x}\text{Ba}_x\text{O}_{2.2}$ ( $0.00 \leq x \leq 0.06$ ) solid solution	67
4.13	The summary for the crystallite sizes and internal strain for $\text{Bi}_{1.2}\text{Sr}_{0.4-x}\text{Ni}_x\text{O}_{2.2}$ ( $0.00 \leq x \leq 0.10$ ) solid solutions	68
4.14	Summary of conductivity and activation energy for $\text{Bi}_{1.2}\text{Sr}_{0.4-x}\text{Mg}_x\text{O}_{2.2}$ ( $0.00 \leq x \leq 0.10$ ) solid solutions	91
4.15	Summary of conductivity and activation energy for $\text{Bi}_{1.2}\text{Sr}_{0.4-x}\text{Ca}_x\text{O}_{2.2}$ ( $0.00 \leq x \leq 0.08$ ) solid solutions	91
4.16	Summary of conductivity and activation energy for $\text{Bi}_{1.2}\text{Sr}_{0.4-x}\text{Ba}_x\text{O}_\delta$ ( $0.00 \leq x \leq 0.06$ ) solid solutions	91
4.17	Summary of conductivity and activation energy for $\text{Bi}_{1.2}\text{Sr}_{0.4-x}\text{Ni}_x\text{O}_\delta$ ( $0.00 \leq x \leq 0.10$ ) solid solution	92



## LIST OF FIGURES

Figure	Page
1.1 Solid electrolytes as an intermediate between normal crystalline solids and liquids (West, 1999)	2
1.2 The ionic conductivity of some of the most promising oxide ion conductors as a function of the inverse temperature (Stephen and Kilner, 2003)	4
1.3 The Schottky and Frenkel defects	5
1.4 Operating principle of Solid Oxide Fuel Cells (Subhash, 2007)	6
2.1 Structure models for fluorite related $\delta$ - $\text{Bi}_2\text{O}_3$ : (a) Sillen models; (b) Gattow models; (c) Willis model (Harwig, 1978)	11
2.2 The stable and metastable regions found in $\text{Bi}_2\text{O}_3$ (Shuk <i>et al.</i> : 1996)	12
2.3 Electrical conductivity of $\text{Bi}_2\text{O}_3$ as function of temperature (Shuk, 1996)	13
2.4 Conductivities of $(\text{Bi}_2\text{O}_3)_{1-x}(\text{SrO})_x$ (Takashi <i>et al.</i> , 1972)	16
3.1 Summary for the preparation of bismuth strontium oxide solid solutions	23
3.2 Summary of preparation and characterization	25
3.3 Impedance diagram due to blocking interface: (a) a perfectly smooth interface; (b) rough electrode or due to Warburg impedance (Armstrong and Todd, 1995)	28
3.4 $Z''$ and $M''$ spectroscopic plot respective to a complex impedance plot for non-homogenous materials	31
4.1 The X-ray diffraction patterns for $\text{Bi}_{2-2x}\text{Sr}_x\text{O}_{3-2x}$ ( $0.1 \leq x \leq 0.6$ ) solid solution	34
4.2 Variation of lattice parameter, (a) ( $a=b$ ) and (b) $c$ for $\text{Bi}_{2-2x}\text{Sr}_x\text{O}_{3-2x}$ ( $0.1 \leq x \leq 0.4$ ) solid solutions	36
4.3 Williamson-Hall plots with five intense X-ray diffraction planes	38
4.4 Comparison of crystallite sizes between Scherrer, Williamson-Hall methods and internal strain	49
4.5 SEM images for $\text{Bi}_{2-2x}\text{Sr}_x\text{O}_{3-2x}$ ( $0.1 \leq x \leq 0.4$ ) solid solutions	41

4.6	Cole-cole plot for $\text{Bi}_{2-2x}\text{Sr}_x\text{O}_{3-2x}$ ( $0.1 \leq x \leq 0.4$ ) solid solution at $200^\circ\text{C}$	42
4.7	Cole-cole plot for $\text{Bi}_{1.2}\text{Sr}_{0.4}\text{O}_{2.2}$ as a function of temperature	44
4.8	Imaginary part of impedance plots, ( $Z''$ ) of $\text{Bi}_{1.2}\text{Sr}_{0.4}\text{O}_{2.2}$ as a function of frequency at different temperatures	45
4.9	Combined $Z''$ and $M''$ spectroscopic plot for $\text{Bi}_{1.2}\text{Sr}_{0.4}\text{O}_{2.2}$ as a function of frequency at $150^\circ\text{C}$	45
4.10	Real admittance plots, $Y''$ as a function of frequency at various temperatures for $\text{Bi}_{1.2}\text{Sr}_{0.4}\text{O}_{2.2}$	46
4.11	Arrhenius conductivity plots of $\text{Bi}_{2-2x}\text{Sr}_x\text{O}_{3-2x}$ where $0.1 \leq x \leq 0.4$ solid solution	48
4.12	The XRD patterns for $\text{Bi}_{1.2}\text{Sr}_{0.4-x}\text{Mg}_x\text{O}_{2.2}$ where ( $0.00 \leq x \leq 0.12$ ) solid solutions	51
4.13	The XRD patterns for of $\text{Bi}_{1.2}\text{Sr}_{0.4-x}\text{Ca}_x\text{O}_{2.2}$ where ( $0.00 \leq x \leq 0.14$ ) solid solutions	52
4.14	The XRD patterns for $\text{Bi}_{1.2}\text{Sr}_{0.4-x}\text{Ba}_x\text{O}_{2.2}$ where ( $0.00 \leq x \leq 0.10$ ) solid solutions	53
4.15	The XRD patterns for $\text{Bi}_{1.2}\text{Sr}_{0.4-x}\text{Ni}_x\text{O}_{2.2}$ where ( $0.00 \leq x \leq 0.12$ ) solid solutions	54
4.16	Variation of lattice parameter (a) ( $a=b$ ) and (b) c as a function of composition in $\text{Bi}_{1.2}\text{Sr}_{0.4-x}\text{Mg}_x\text{O}_{2.2}$ ( $0.00 \leq x \leq 0.10$ ) solid solutions	56
4.17	Variation of lattice parameter (a) ( $a=b$ ) and (b) c as a function of composition in $\text{Bi}_{1.2}\text{Sr}_{0.4-x}\text{Ca}_x\text{O}_{2.2}$ ( $0.00 \leq x \leq 0.08$ ) solid solutions	57
4.18	Variation of lattice parameter (a) ( $a=b$ ) and (b) c as a function of composition in $\text{Bi}_{1.2}\text{Sr}_{0.4-x}\text{Ba}_x\text{O}_{2.2}$ ( $0.00 \leq x \leq 0.06$ ) solid solutions	57
4.19	Variation of lattice parameter (a) ( $a=b$ ) and (b) c as a function of composition in $\text{Bi}_{1.2}\text{Sr}_{0.4-x}\text{Ni}_x\text{O}_{2.2}$ ( $0.00 \leq x \leq 0.10$ ) solid solutions	58
4.20	W-H plots for $\text{Bi}_{1.2}\text{Sr}_{0.4-x}\text{Mg}_x\text{O}_{2.2}$ ( $0.00 \leq x \leq 0.10$ ) solid solutions	59
4.21	Comparison between crystallite sizes, D calculated by (1) Scherrer (2) William-son Hall methods and the internal strains $\text{Bi}_{1.2}\text{Sr}_{0.4-x}\text{Mg}_x\text{O}_{2.2}$ ( $0.00 \leq x \leq 0.10$ ) solid solutions	60
4.22	W-H plots for $\text{Bi}_{1.2}\text{Sr}_{0.4-x}\text{Ca}_x\text{O}_{2.2}$ ( $0.00 \leq x \leq 0.08$ ) solid solutions	60
4.23	Comparison between crystallite sizes, D calculated by (1) Scherrer (2) William-son Hall methods and the internal strains	

	$\text{Bi}_{1.2}\text{Sr}_{0.4-x}\text{Ca}_x\text{O}_2$ ( $0.00 \leq x \leq 0.08$ ) solid solutions	61
4.24	W-H plots for $\text{Bi}_{1.2}\text{Sr}_{0.4-x}\text{Ba}_x\text{O}_{2.2}$ ( $0.00 \leq x \leq 0.06$ ) solid solution	62
4.25	Comparison between crystallite sizes, D calculated by (1) Scherrer (2) William-son Hall methods and the internal strains $\text{Bi}_{1.2}\text{Sr}_{0.4-x}\text{Ba}_x\text{O}_{2.2}$ ( $0.00 \leq x \leq 0.06$ ) solid solution	63
4.26	W-H plots for $\text{Bi}_{1.2}\text{Sr}_{0.4-x}\text{Ni}_x\text{O}_{2.2}$ ( $0.00 \leq x \leq 0.10$ ) solid solutions	63
4.27	Comparison between crystallite sizes, D calculated by (1) Scherrer (2) William-son Hall methods and the internal strains $\text{Bi}_{1.2}\text{Sr}_{0.4-x}\text{Ni}_x\text{O}_{2.2}$ ( $0.00 \leq x \leq 0.10$ ) solid solutions	64
4.28	SEM images of $\text{Bi}_{1.2}\text{Sr}_{1-x}\text{Mg}_x\text{O}_{2.2}$ ( $0.00 \leq x \leq 0.10$ ) solid solution at 3K magnification	69
4.29	SEM images of $\text{Bi}_{1.2}\text{Sr}_{1-x}\text{Ca}_x\text{O}_{2.2}$ ( $0.00 \leq x \leq 0.08$ ) solid solution at 3K magnification	70
4.30	SEM images of $\text{Bi}_{1.2}\text{Sr}_{1-x}\text{Ba}_x\text{O}_{2.2}$ ( $0.00 \leq x \leq 0.06$ ) solid solution at 3K magnification	71
4.31	SEM images of $\text{Bi}_{1.2}\text{Sr}_{1-x}\text{Ni}_x\text{O}_{2.2}$ ( $0.00 \leq x \leq 0.10$ ) solid solution at 3K magnification	72
4.32	Cole-cole plot for $\text{Bi}_{1.2}\text{Sr}_{0.4-x}\text{Mg}_x\text{O}_{2.2}$ ( $0.00 \leq x \leq 0.10$ ) solid solutions	73
4.33	Cole-cole plot for $\text{Bi}_{1.2}\text{Sr}_{0.4-x}\text{Ca}_x\text{O}_{2.2}$ ( $0.00 \leq x \leq 0.08$ ) solid solutions	74
4.34	Cole-cole plot for $\text{Bi}_{1.2}\text{Sr}_{0.4-x}\text{Ba}_x\text{O}_{2.2}$ ( $0.00 \leq x \leq 0.06$ ) solid solutions	74
4.35	Cole-cole plot for $\text{Bi}_{1.2}\text{Sr}_{0.4-x}\text{Ni}_x\text{O}_{2.2}$ ( $0.00 \leq x \leq 0.10$ ) solid solutions	75
4.36	Cole-cole plot for $\text{Bi}_{1.2}\text{Sr}_{0.3}\text{Mg}_{0.1}\text{O}_{2.2}$	76
4.37	Cole-cole plot for $\text{Bi}_{1.2}\text{Sr}_{0.32}\text{Ca}_{0.08}\text{O}_{2.2}$	76
4.38	Cole-cole plot for $\text{Bi}_{1.2}\text{Sr}_{0.38}\text{Ba}_{0.02}\text{O}_{2.2}$	77
4.39	Cole-cole plot for $\text{Bi}_{1.2}\text{Sr}_{0.3}\text{Ni}_{0.1}\text{O}_{2.2}$	77
4.40	Imaginary part of impedance plots, ( $Z''$ ) of $\text{Bi}_{1.2}\text{Sr}_{0.3}\text{Mg}_{0.1}\text{O}_{2.2}$ as a function of frequency at different temperatures	78
4.41	Imaginary part of impedance plots, ( $Z''$ ) of $\text{Bi}_{1.2}\text{Sr}_{0.32}\text{Ca}_{0.08}\text{O}_{2.2}$ as a function of frequency at different temperatures	79
4.42	Imaginary part of impedance plots, ( $Z''$ ) $\text{Bi}_{1.2}\text{Sr}_{0.38}\text{Ba}_{0.02}\text{O}_{2.2}$ as a function of frequency at different temperatures	79

4.43	Imaginary part of impedance plots, ( $Z''$ ) of $\text{Bi}_{1.2}\text{Sr}_{0.3}\text{Ni}_{0.1}\text{O}_{2.2}$ as a function of frequency at different temperatures	80
4.44	Imaginary part of impedance plots, ( $Z''$ ) and $M''$ for $\text{Bi}_{1.2}\text{Sr}_{0.3}\text{Mg}_{0.1}\text{O}_{2.2}$ as a function of frequency at temperature of $200^\circ\text{C}$	81
4.45	Imaginary part of impedance plots, ( $Z''$ ) and $M''$ for $\text{Bi}_{1.2}\text{Sr}_{0.32}\text{Ca}_{0.08}\text{O}_{2.2}$ as a function of frequency at temperature of $200^\circ\text{C}$	82
4.46	Imaginary part of impedance plots, ( $Z''$ ) and $M''$ for $\text{Bi}_{1.2}\text{Sr}_{0.38}\text{Ba}_{0.02}\text{O}_{2.2}$ as a function of frequency at temperature of $200^\circ\text{C}$	83
4.47	Imaginary part of impedance plots, ( $Z''$ ) and $M''$ for $\text{Bi}_{1.2}\text{Sr}_{0.3}\text{Ni}_{0.1}\text{O}_{2.2}$ as a function of frequency at temperature of $200^\circ\text{C}$	84
4.48	Real admittance plots, $Y'$ $\text{Bi}_{1.2}\text{Sr}_{0.3}\text{Mg}_{0.1}\text{O}_{2.2}$ as a function of frequency at various temperature	85
4.49	Real admittance plots, $Y'$ $\text{Bi}_{1.2}\text{Sr}_{0.32}\text{Ca}_{0.08}\text{O}_{2.2}$ as a function of frequency at various temperature	85
4.50	Real admittance plots, $Y'$ $\text{Bi}_{1.2}\text{Sr}_{0.38}\text{Ba}_{0.02}\text{O}_{2.2}$ as a function of frequency at various temperature	86
4.51	Real admittance plots, $Y'$ $\text{Bi}_{1.2}\text{Sr}_{0.3}\text{Ni}_{0.1}\text{O}_{2.2}$ as a function of frequency at various temperature	86
4.52	Arrhenius plots for $\text{Bi}_{1.2}\text{Sr}_{0.4-x}\text{Mg}_x\text{O}_{2.2}$ ( $0.00 \leq x \leq 0.10$ ) solid solutions	89
4.53	Arrhenius plots for $\text{Bi}_{1.2}\text{Sr}_{0.4-x}\text{Ca}_x\text{O}_{2.2}$ ( $0.00 \leq x \leq 0.08$ ) solid solutions	89
4.54	Arrhenius plots for $\text{Bi}_{1.2}\text{Sr}_{0.4-x}\text{Ba}_x\text{O}_{2.2}$ ( $0.00 \leq x \leq 0.06$ ) solid solutions	90
4.55	Arrhenius plots for $\text{Bi}_{1.2}\text{Sr}_{0.4-x}\text{Ni}_x\text{O}_{2.2}$ ( $0.00 \leq x \leq 0.10$ ) solid solutions	90

## LIST OF ABBREVIATIONS

ac	alternating current
ICDD	international centre for diffraction data
SEM	scanning electron microscopy
SOFC	solid oxide fuel cells
XRD	x-ray diffraction
YSZ	yttria stabilized zirconia
a,b,c	lattice diffraction
A	area
C	capacitance
E <sub>a</sub>	activation energy
M'	real part modulus
M''	imaginary part of modulus
R	resistance
Z	impedance
Z'	real part impedance
Z''	imaginary part of impedance
Z*	complex impedance
J	flux of charge
J	density of the current
$\lambda$	wavelength
E	electric field
T	temperature
L	length
$\epsilon$	permittivity

$\epsilon'$	relative permittivity
f	frequency
$\sigma$	conductivity
$\theta$	angle
Å	Angstrom unit
eV	electron volt unit
K	kelvin unit
K	Boltzman's constant
$\omega$	angular frequency
$\epsilon_0$	pre exponential factor



© COPYRIGHT UPM

## CHAPTER 1

### INTRODUCTION

#### 1.1 Overview

In recent years, the rapid growth of modern communication technologies and electronic device has drawn much research interest in high performance functional materials. Oxides with diverse electrical properties are greatly demanded for various uses. The interest in oxide-ion conductor increases and pace of research on oxide-ion conductors has been rapid ever since their discovery by Faraday over 200 years ago. This is because of their potential applications in various important technological devices such as solid oxide fuel cells (SOFC's). Such device converts the chemical energy of fuel cells directly into electricity and heat by electrochemically combining the fuel and oxidant gas via an ion conducting electrolyte (Tan *et al.*, 2012). The advantages of SOFC's include high efficiency, long-term stability, fuel flexibility, low emissions and relatively low cost.

Ceramics oxides, such as yttria-stabilized zirconia (YSZ), have been used as electrolytes together with composite powder mixtures, e.g. nickel oxide (NiO) as anode materials in SOFC's. The YSZ is widely used because of its sufficient ionic conductivity, chemical stability and mechanical strength. This material is having conductivity about  $0.1 \text{ Scm}^{-1}$  at temperature of 1273K and thus need to be operated at high temperature. Therefore, heat evolved in the fuel cells can be used in the reforming process when operate at high temperature. However, several issues were detected as a drawback to this high operating temperature. One of the most important issues is the thermal stress caused from the thermal expansion coefficient mismatch and the temperature distribution developed inside the cells. Scandium, Sc was discovered to replace the yttrium, Y in YSZ and scandia-doped zirconia was found to have higher conductivity than YSZ. However, higher cost of scandium and detrimental ageing effects in scandia-doped  $\text{ZrO}_2$  make it less attractive in commercializing SOFC's (Singhal, 2007). Meanwhile, alternative anode materials, typically containing transition metals such as Co, Fe and/or Ni were develop and optimized for better performance. In general, these materials offer higher oxide ion diffusion rates and exhibit faster oxygen reduction kinetics. However, the thermal expansion coefficient of cobaltites is much higher than that of YSZ electrolyte, and the electrical conductivities of ferrites and nickelites are low. These materials are found to have a decrease in conductivities during cell lifetime as a result of chemical or microstructure instability. New materials with higher oxide ion conduction and better stability are required for SOFC's and most other oxide ion conductor related devices in order to overcome these disadvantages and enhance device efficiency.



## 1.2 Solid Electrolytes

Solid electrolytes are materials that conduct electricity by the motion of ions of rapid diffusion and exhibit negligible electronic transport. One component of the structure either cationic or anionic is not confined to specific lattice sites in solid electrolytes. However, it is essentially free to move throughout the structure but restricted only for one species mobile. Such materials are often having rather special crystal structure with open tunnels or layers through which the mobile ions may move around (West, 1999). Therefore, solid electrolytes must have the characteristics of large number of mobile cation and anions, which requires a large number of empty sites, either the vacancies or accessible interstitial sites. The empty and occupied sites have similar potential energies with low activation energy barrier for jumping between neighboring sites as the high activation energy will decrease the carrier mobility, very stable sites lead to carrier localization. Other than that, the migration of the lattice should be in “molten”, as the other ions of the solid framework (like 3D with permeated open channel) must prevent the entire material from being melted. The framework ions are required to be highly polarizable in order to stabilize the transition state of geometries of the migrating ions through the covalent interactions (West, 1984).

Solid electrolyte is known as an intermediate between normal crystalline solids and liquid as could be seen in Figure 1.1. It possesses properties of normal crystalline solid with regular three-dimensional structures and liquid electrolyte with irregular structure but with mobile ions. Their conductivity values are comparable to strong liquid electrolytes. The uses of solid electrolytes have more advantages than the liquid electrolytes. This is because solid electrolytes have longer lifetime, high energy density, and low possibility of leaking compared to liquid electrolytes. Thus, there is great interest in studying the properties of solid electrolytes and their usage in solid state electrochemical devices.

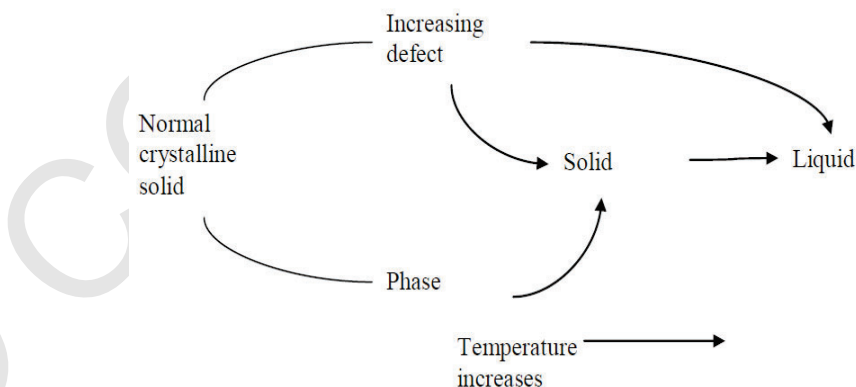


**Figure 1.1: Solid electrolytes as an intermediate between normal crystalline solids and liquids (West, 1999)**

### 1.3 Oxide Ion Conductors

Oxide ion conducting solid electrolytes play an important role in electrochemical cells for measuring oxygen activities and thermodynamic data of solid, liquid, and gaseous phases. Oxide ion conductivity generally occurs through oxygen vacancy which could be introduced by doping aliovalent cation. No ion can diffuse except for interstitial position for the case of perfect crystals which means no defects but vacancy can diffuse. The typical theory for ion diffusion is treated with random theory, in which diffusion of vacancy is strongly related with the jump frequency and the number of jump site. Thus, the diffusivity of oxygen vacancy is strongly related to the crystal structure and dopants.

### 1.4 Ionic Conductivity

The ionic conductivity is strongly temperature dependent, but at high temperature can approach value close to  $1 \text{ Scm}^{-1}$  ( $\log \sigma$  axis) comparable to the levels of ionic conductivity found in liquid electrolytes as could be seen in Figure 1.2. The BICUVOX.10 shows the highest conductivity as compared to others and as temperature increases to  $800^\circ\text{C}$ , the conductivity is approximately  $1 \text{ Scm}^{-1}$ . Therefore, support the idea that the conductivity is strongly temperature dependent. The requirements for the ionic conduction to occur are the crystal must contain unoccupied sites equivalent to those occupied by the lattice oxygen ions. Secondly, the energy involved in the process of migration from one site to the unoccupied equivalent site must be small, certainly less than about 1 eV.

Ionic conductivity is closely related to the presence of defects or disordered structure which indicates a multiplicity of positions in the crystal structure that can be replaced by certain type of ion. The structure itself must have a character which tolerates ion diffusion. Substances with high ionic conductivity can be categorized into four groups, as substance with thermally induced defects, impurity-induced defects, crystal structure disorder and amorphous character (Koller, 1994). Two types of defects are important for the ion mobility in crystals which are "Schottky" and "Frenkel" defects. Schottky defect is the crystal imperfection in which pairs of ions, one cation and the other an anion disappears leaving their position vacant. Meanwhile, Frenkel defect is a single ion missing from its regular position and wandering in the interstitial sites. Both Frankel and Schottky defects form a vacant site in the crystal and any ion in the intermediate vicinity can jump to one of the vacant site. Therefore, previous site of the ion vacant could be host by another ion, hence leading to transport of the ions across the solid and give rise in conductivity. Figure 1.3 shows the illustration for the Shottky and Frenkel defects.

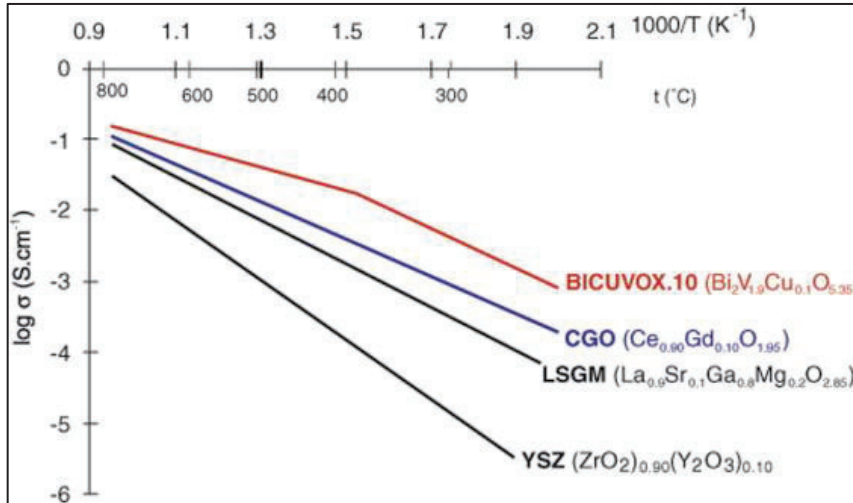


**Figure 1.2: The ionic conductivity of some of the most promising oxide ion conductors as a function of the inverse temperature (Stephen and Kilner, 2003)**

The density of defects, which is the number of defects per unit volume in a crystal, depends on various factors such as the structure, temperature, the presence of impurity ion, and the nature of chemical bonding between the constituent ions. The ionic solids can be classified based on the type of defect or disorder responsible for ionic conduction. Roth and Rice classified the crystalline ionic conductors based on:

**Type I:** Ionic solids with low concentration of defects  $\sim 10^{18} \text{ cm}^{-3}$  at room temperature. These are generally poor ionic conductors such as NaCl and KCl.

**Type II:** Ionic solids with high concentration of defects  $\sim 10^{20} \text{ cm}^{-3}$  at room temperature. These are good ionic conductors at room temperature and fast ion conductors at high temperature. For examples are the  $\text{ZrO}_2$  and  $\text{CaF}_2$ .

**Type III:** Solids have a “molten” sub-lattice or “liquid-like” structure of the mobile ions with the concentration of  $\sim 10^{22} \text{ cm}^{-3}$ . The  $\text{RbAg}_4\text{I}_5$  and Na- $\beta$ -alumina are examples.

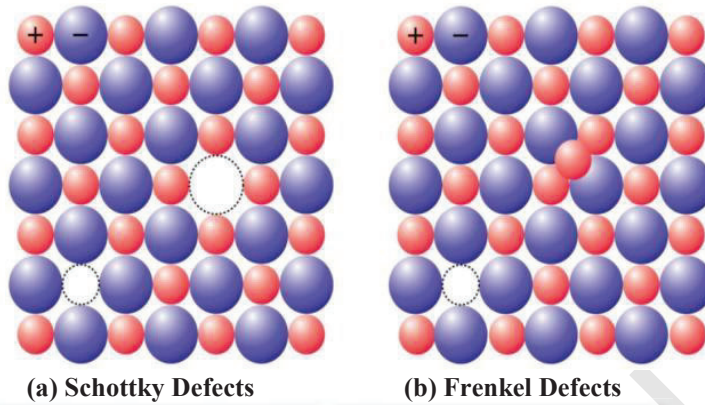


**Figure 1.3: The Schottky and Frenkel defects**

### 1.5 Application of Ionic Conduction

Studies of fast ionic conductors are important due to the use in the construction of technologically useful devices. One of the applications is that the construction of the electrochemical cell which used for the energy conversion or energy storage like the primary and secondary batteries. The other applications are the oxygen monitors, which used to provide efficient control of combustion, and the high temperature of fuel cell, which used to convert chemical to electrical energy in the solid oxide fuel cells (SOFC).

For example, the stabilized zirconia discovered to be the oxygen ion conductors and remain as one of the best conductors. Large concentration of oxide ion vacancies,  $V_o$  can be obtained in the crystal lattice of  $ZrO_2$  if lower valent metal ions are substituted for  $Zr^{4+}$  in  $ZrO_2$ .



where  $M_{Zr}''$  is a  $M^{2+}$  -ion in a  $Zr^{4+}$  lattice site and  $O_o^X$  is an  $O^{2-}$  -ion on a regular lattice site.

#### 1.5.1 Solid Oxide Fuel Cells (SOFC's)

An SOFC essentially consists of two porous electrodes separated by a dense, oxide ion conducting electrolyte. Oxygen supplied at the cathode (air electrode) reacts with

incoming electrons from the external circuit to form oxide ions, which migrate to the anode (fuel electrode) through the oxide ion conducting electrolyte. At the anode, oxide ions combine with H<sub>2</sub> (and/or CO) in the fuel to form H<sub>2</sub>O (and/or CO<sub>2</sub>), liberating electrons. Electrons (electricity) flow from the anode through the external circuit to the cathode. The materials for the cell components are selected based on suitable electrical conducting properties required of these components to perform their intended cell functions; adequate chemical and structural stability at high temperatures encountered during cell operation as well as during cell fabrication; minimal reactivity and inter-diffusion among different components; and matching thermal expansion among different components (Subhash, 2007) as shown in Figure 1.4. The SOFC's normally operate at high temperature of 800°C-1000°C.

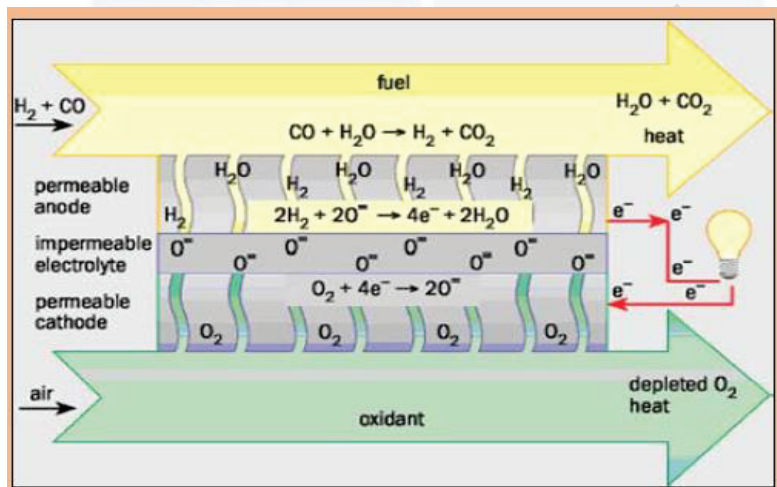


Figure 1.4: Operating principle of Solid Oxide Fuel Cells (Subhash, 2007)

Solid oxide fuel cells (SOFC) are the environmentally friendly energy conversion systems to produce the electrical energy with minimal environmental damage. The other advantages are high power density, high energy-conversion efficiency, and lower emission of CO<sub>2</sub>, CO, NO<sub>x</sub>, SO<sub>2</sub>, and fuel flexibility. Most of the electrochemical reactions occur at three-phase boundaries (TPB), which are defined as the sites where the ionic, electronic conductor and the gas phase are in contact i.e. where the electrode, the electrolyte and the gas phase are in contact. TPB characteristics have a large influence on the electrochemical performance of cell. The electrochemical reactions that fuel cells use to produce electricity occur in the presence of these three phases, so the triple phase boundaries can be thought of as the active areas of the cell. The oxygen reduction reaction that occurs at a solid oxide fuel cell's cathode, can be written as follows:





Different mechanisms bring these reactants to a TPB to carry out this reaction. The kinetics of this reaction is one of the limiting factors in cell performance, so increasing the TPB density will increase the reaction rate, and thus increase cell performance.

The electrochemical reduction of oxygen occurs at the cathode SOFC electrode. The cathode must have adequate porosity to allow oxygen diffusion, chemical compatibility with the other contacting components under operating conditions, a thermal expansion coefficient (TEC) matching those of another components, chemical and microstructure stability under an oxidizing atmosphere during fabrication and operation, low cost and relatively simple fabrication procedure, high catalytic activity for the oxygen reduction reaction, large TPB, adhesion to electrolyte surface and high electronic and ionic conductivity.

While, the characteristics needed for the anode are: (1) the high electrical conductivity, (2) a thermal expansion coefficient, TEC that matches those of the adjoining components, (3) the capacity to avoid coke deposition, (4) fine particle size, (5) chemical compatibility with another cell components under reducing atmosphere at the operating temperature, (6) large TPB, (7) high electrochemical or catalytic activity for the oxidation of the selected fuel gas, (8) high porosity for the fuel supply and reaction product removal, (9) good electronic and ionic conductive phases. The Ni/YSZ is a common anode used for the SOFC.

The electrolyte needs to have characteristic of oxide-ion conductivity greater than  $10^{-2} \text{ Scm}^{-1}$  at the operating temperature, negligible electronic conduction, high density to promote the gas impermeability, thermodynamically stable, TEC compatible, suitable mechanical properties and negligible chemical interaction with electrode materials under operation and fabrication conditions. Most of the high temperature fuel cells operate via oxygen ion ( $\text{O}^{2-}$ ) conduction from the air electrode to the fuel electrode. This conduction occurs because of the presence of oxygen ions vacancies, so the crystallites forming the electrolyte must have unoccupied anionic sites. The energy required for the oxide ion migration from one site to the neighboring unoccupied equivalent site must be small (Faro *et al.*, 2009).

## 1.6 Problem Statements

Yttria stabilized zirconia (YSZ) which is used as the electrolyte in SOFC operates at high temperature around  $1000^{\circ}\text{C}$ . Thus, high operating temperatures will result in high fabrication costs and also affect the material stability and compatibility and the thermal degradation of the electrolyte itself. Therefore, there is a continuing effort to search for oxide ion conductors that can operate at lower temperature in order to reduce costs.

The sintered oxides which consisted of  $\text{Bi}_2\text{O}_3$  and SrO was found to have high oxide ion conductivity even at relatively lower temperature. The  $\text{Bi}_2\text{O}_3$ -SrO system forms rhombohedral solid solutions in the composition range between 20 and 45 mole% SrO which contains 2.5 ~ 5.4 of oxide ion vacancies per 18 lattice sites of oxide ion in the

unit cell. However, the investigation on the electrical conduction on this material is yet limited.

In this thesis, more focus on structure and electrical properties of the bismuth strontium which has been systematically studied due to less well understood and analysis of this material. The strontium ion is used as it has high polarizability that is expected to enhance the electrical properties (conductivity). The divalent dopants (Mg, Ca, Ba and Ni) were chosen to replace some of the strontium site. The criteria considered in selecting the suitable dopant is the comparable ionic radii of the replacing and replacable cations or else lead to high internal strain or structural disorder (Mat Dasin, 2017).

### 1.7 Objectives

The objectives of this study are:

1. To prepare the solid solution of bismuth strontium oxide,  $\text{Bi}_{2-2x}\text{Sr}_x\text{O}_{3+2x}$  and its doped materials using solid state method.
2. To characterize bismuth strontium based solid solutions using the X-ray diffraction analysis (XRD), energy dispersive X-ray (EDX), and Scanning Electron Microscopy (SEM).
3. To evaluate the electrical properties of single phase materials using AC impedance spectroscopy.

## REFERENCES

- Badwal, S.P.S (2001), Stability of solid oxide fuel cell components, *Solid state Ionics*, vol.143, No.1-4 (June 2001), pp.39-46
- Bruce, P. (eds), (1995), *Solid state electrochemistry* (New York: Cambridge University Press),
- Battle P.D., Catlow C.R.A., Drennan J., Murray A.D., (1983), The structural properties of cubic zinc tantalite, *Ceramics International* 35, 1473-1480
- Buchi Suresh M. Johnson Roy (2012), The effect of strontium doping on densification and electrical properties of  $\text{Ce}_{0.8}\text{Gd}_{0.2}\text{O}_{2-\delta}$  electrolyte for IT-SOFC application, *Solid State Ionics* 18:291–297.
- Boivin, J.C., and Thomas, D.J., (1981) Structural investigations on bismuth-based mixed oxide, *Solid State Ionics* 3/4: 457-462.
- Chandra, S., (1981) Superionic solid principles and application (Amsterdam: North-Holland).
- Coondoo, I., (2007) Investigations of structural, dielectric and ferroelectric behavior of europium substituted  $\text{SrBi}_2\text{Ta}_2\text{O}_9$  ferroelectric ceramics, *Solid State Communications* 142 561-565
- Coondoo, I., (2007) Structural, dielectric and electrical studies in tungsten doped  $\text{SrBi}_2\text{Ta}_2\text{O}_9$  ferroelectric ceramics, *Ceramics International* 33 41-47
- Chon, M.P., Tan, K.B., Khaw, C.C., Zainal, Z., Taufiq-Yap, Y., Chen, S.K. and Tan, Y.P. (2014). Investigation of the phase formation and dielectric properties of  $\text{Bi}_7\text{Ta}_3\text{O}_{18}$ . *Journal of Alloys and Compounds*, 590; 479-485.
- Chon, M.P., Tan, K.B., Khaw, C.C., Zainal, Z., Taufiq-Yap, Y., Chen, S.K. and Tan, P.Y. (2016). Synthesis and electrical properties of Zn-substituted bismuth copper tantalite pyrochlores, *International Journal Applied Ceramic Technology*, 13 (4) 718-725.
- D.Dhak et al., (2008) Influence of substitution on dielectric and impedance spectroscopy of  $\text{Sr}_{1-x}\text{Bi}_{2+y}\text{Nb}_2\text{O}_9$  ferroelectric ceramics synthesized by chemical route, *Applied Surface Science* 254 3078-3092.
- Faraday, M. Philos. Trans. R. Soc. London (London: Richard and J. Taylor) 1838
- Fergus, J.; Hui, Rob.; Li, X.; Wilkinson, D.P.; Zhang, J. Jeffrey (Ed(s)) (2009) Solid oxide fuel cells: material properties and performance .



- Firman, K., Tan, K.B., Khaw, C.C., Zainal, Z., Tan, Y.P., and Chen, S.K., (2017) Doping mechanisms and electrical properties of bismuth tantalate fluorites, *Journal Material Science* 52:10106–10118.
- Fruth, V., Ianculescu, A., Berger, D., Preda, S., Voicu, G., Tenea, E., and Popa, M., (2006) Synthesis, structure and properties of doped Bi<sub>2</sub>O<sub>3</sub>, *Journal of European Ceramic Society* 26; 311-3016.
- Harwig, H.A. (1978). On the structure of bismuthsesquioxide: the  $\alpha$ ,  $\beta$ ,  $\gamma$  and  $\delta$ -phase. *Zeitschrift für Anorganische und Allgemeine Chemie*, 444: 265-274.
- Irvine, J.T., Sinclair, D.C. and West, A.R. (1990). Electroceramics: characterization by impedance spectroscopy. *Advanced Materials*, 2: 132-138.
- Khaw, C.C., Tan, K.B., Lee, C.K., (2009), High temperature dielectric properties of cubic zink tantalite, *Ceramics International* 35, 1473-1480.
- Levin, E.M., and Roth., R.S., (1964). Polymorphism of bismuth sesquioxide.II. Effect of the additions on the polymorphism of Bi<sub>2</sub>O<sub>3</sub>. *Journal of Research of the National Bureau of Standards-A. Physics and Chemistry*, 68A: 197-206.
- Mat Dasin, N.A., (2017) Subsolidus solution and electrical properties of Sr-substituted bismuth magnesium niobate pyrochlores, *Ceramics International*.
- Marcurio, D., Champarnaud, J.C., Mesjard and Frit, B., (1994) Thermal Evolution of the Crystal Structure of the Rhombohedral Bi<sub>0.75</sub>Sr<sub>0.25</sub>O<sub>1.375</sub> Phase: A Single Crystal Neutron Diffraction Studies; *Journal of Solid State Chemistry*, 112, 1-8.
- Naixiong Jiang, Eric D.Wachsman, Su-Ho Jung, (2002), A Higher Conductivity of Bi<sub>2</sub>O<sub>3</sub>-based Electrolyte; *Solid State Ionics* 150, 347-353.
- Ng, S.N., Tan, Y.P. and Taufiq-Yap, Y.H., (2008) Preparation and Characterization of Bismuth-Niobium Oxide Ion Conductors, *Solid State Science and Technology*, Vol.16, No 1: 205-214.
- Ng, S.N., Tan, Y.P. and Taufiq-Yap, Y.H., (2009) Mechanochemical Synthesis and Characterisation of Bismuth-Niobium Oxide Ion Conductors, *Journal of Physical Chemistry B*, Vol 20(I): 75-86.
- Payzan, E.A., Porter, W.D., and Hubbard. C.R. (1998) High temperature phase transformation in rhombohedral bismuth strontium oxide, *Thermochimica Acta* 318: 45-50.
- Sakshi Gupta and Singh, K., (2015) Effect of two different dopants (Mg<sup>2+</sup> and Ca<sup>2+</sup>) and processing parameters on  $\gamma$ -phase stabilization and conductivity of Bi<sub>4</sub>V<sub>2</sub>O<sub>11- $\delta$</sub> , *Ceramics International* 41: 9496-9504.

- Sinclair, C., and West, A.R., (1989) 'Impedance and modulus spectroscopy of semiconducting BaTiO<sub>3</sub> showing positive temperature coefficient of resistance,' *Journal of Applied Physics*, Vol 66, pp.3850-3856.
- Shuk,P., Wiemhofer, H.D., Guth, U., Gopel, W. and Greenblatt, M., (1996). Oxide ion conducting solid electrolytes based on Bi<sub>2</sub>O<sub>3</sub>. *Solid State Ionics*, 89: 179-196.
- Singhal,S.C.& Kendall,K, (2003) High temperature solid oxide fuel cells: fundamental design, and applications .
- Sun,C.; Hui,R.;Roller,J.(2010) Cathode materials for solid oxide fuel cells. *J solid state electrochem*, vol.14, No.7, (July 2010), pp. (1125-1144)
- S.O'Brien et.al., (2006) Structural and electrical characterization of strontium bismuth tantalate (SBT) thin film, *Applied Surface Science* 252 4497-4501
- Tan, K.B., Khaw, C.C., Lee, C.K., Zainal, Z., Tan, Y.P., and Shaari, H. (2009) High temperature impedance spectroscopy study of non-stoichiometric bismuth zinc niobate pyrochlore, *Materials Science-Poland*, Vol.27, No.4/1.
- Tan, M.Y., Tan, K.B., Zainal, Z., Khaw, C.C.,Chen, S.K., (2012) Subsolidus formation and impedance spectroscopy studies of materials in the (Bi<sub>2</sub>O<sub>3</sub>)<sub>1-x</sub> (Y<sub>2</sub>O<sub>3</sub>)<sub>x</sub> binary system, *Ceramics International* 38, 3403-3409.
- Takashi, T. and Iwahara, H. (1978). Oxide ion conductors based on bismuthsesquioxide. *Materials Research Bulletin*, 13: 1447-1453.
- Takashi, T., Iwahara, H., and Nagai, Y., (1972) High Oxide Ion Conduction in Sintered Bi<sub>2</sub>O<sub>3</sub> containing SrO, CaO or La<sub>2</sub>O<sub>3</sub>; *Journal of Applied Electrochemistry* 2.
- Tan K.B., Chon M.P., Khaw C.C., Zainal Z., Taufiq-Yap Y.H., Tan P.Y., (2014) Novel monoclinic zirconolite in Bi<sub>2</sub>O<sub>3</sub>-CuO-Ta<sub>2</sub>O<sub>5</sub> ternary system: phase equilibria, structural and electrical properties, *Journal of Alloys and Compounds* 592: 140-149.
- Venkataraman, B.H., Varma, K.B.R., (2003) Impedance and dielectric studies of ferroelectric SrBi<sub>2</sub>Nb<sub>2</sub>O<sub>9</sub> ceramics, *Journal of Physics and Chemistry of Solids* 64 2105-2112.
- Vstavskaya, E.Yu., Zuev, A.Yu., and Cherepanow, V.A., (1994) The Bi<sub>2</sub>O<sub>3</sub>-SrO phase diagram, *Journal of Phase Equilibria* Vol. 15 No. 6.
- Wu (2001) Doping effect in layered structure of SrBi<sub>2</sub>Nb<sub>2</sub>O<sub>9</sub> ferroelectrics, *Journal of Applied Physics*, Vol.90, No.10
- West, A.R., (1999). Electrical properties. In basic solid state chemistry, ed.A.R. West, pp 226-311. New York: John Wiley and Sons, Ltd.

Watanabe, A. (1989) Phase stability of  $\text{Bi}_{0.765}\text{Sr}_{0.235}\text{O}_{1.383}$  type bismuth mixed oxides with hexagonal symmetry, *Solid State Ionics* 35: 281-283.

Zhang, F.X., Manoun, B., Saxena S.K., and Zha, C.S., (2006) Structural Behavior of  $\text{Sr}_2\text{Bi}_2\text{O}_5$  at High Pressures, *Journal of Solid State Chemistry*, 179, 544-550.

Z-P.Cao, Piezoelectric properties and thermal stabilities of strontium bismuth titanate ( $\text{SrBi}_4\text{Ti}_4\text{O}_{12}$ ), *Ceramics International* 41 (2015) 13974-13982.

Zhong, G.H., Wang, J.L., and Zeng, Z., (2006) Ionic transport properties in doped  $\delta$ - $\text{Bi}_2\text{O}_3$ , *Journal of Physics*: 106-109.



## BIODATA OF STUDENT

Rohayu binti Mohd Noor was born in Pasir puteh, Kelantan on 5<sup>th</sup> March 1992. She received her early education at Sekolah Kebangsaan Kampong raja. Her secondary education was Sekolah Menengah Kebangsaan Gaal for five years before continue her study at Pulau Pinang Matriculation College for a year (2009). In 2010, she started her higher education at University Putra Malaysia and graduated in year 2015 in Bachelor of Science in Petroleum Chemistry. She then further her Master degree in Materials Chemistry.

